



## Original Research



## PTPN3 is a potential target for a new cancer immunotherapy that has a dual effect of T cell activation and direct cancer inhibition in lung neuroendocrine tumor

Satoko Koga<sup>a,b</sup>, Hideya Onishi<sup>a,\*</sup>, Shogo Masuda<sup>a</sup>, Akiko Fujimura<sup>a</sup>, Shu Ichimiya<sup>a,b</sup>, Kazunori Nakayama<sup>a,b</sup>, Akira Imaizumi<sup>a</sup>, Kenichi Nishiyama<sup>b,c</sup>, Masayuki Kojima<sup>b,c</sup>, Kei Miyoshi<sup>b</sup>, Katsuya Nakamura<sup>d</sup>, Masayo Umabayashi<sup>e</sup>, Takashi Morisaki<sup>e</sup>, Masafumi Nakamura<sup>b</sup>

<sup>a</sup> Department of Cancer Therapy and Research, Graduate School of Medical Sciences, Kyushu University, 3-1-1 Maidashi, Higashi-ku, Fukuoka 812-8582, Japan

<sup>b</sup> Department of Surgery and Oncology, Graduate School of Medical Sciences, Kyushu University, Fukuoka, Japan

<sup>c</sup> Japanese Red Cross Fukuoka Hospital, Fukuoka, Japan

<sup>d</sup> Department of Respiratory Surgery, Japan Community Health Care Organization Kyushu Hospital, Kitakyushu, Japan

<sup>e</sup> Fukuoka General Cancer Clinic, Fukuoka, Japan

## ARTICLE INFO

## Keywords:

PTPN3  
Lung net  
Cancer immunotherapy strategy  
Cancer suppression  
Lymphocyte activation

## ABSTRACT

In our previous study, we found that inhibition of protein tyrosine phosphatase non-receptor type 3 (PTPN3), which is expressed in lymphocytes, enhances lymphocyte activation, suggesting PTPN3 may act as an immune checkpoint molecule. However, PTPN3 is also expressed in various cancers, and the biological significance of PTPN3 in cancer cells is still not well understood, especially for lung neuroendocrine tumor (NET). Therefore, we analyzed the biological significance of PTPN3 in small cell lung cancer and examined the potential for PTPN3 inhibitory treatment as a cancer treatment approach in lung NET including small cell lung cancer (SCLC) and large cell neuroendocrine cancer (LCNEC).

Experiments in a mouse xenograft model using allo lymphocytes showed that PTPN3 inhibition in SCLC cells enhanced the anti-tumor effect of PTPN3-suppressed activated lymphocytes. In addition, PTPN3 was associated with increased vascularization, decreased CD8/FOXP3 ratio and cellular immunosuppression in SCLC clinical specimens. Experiments in a mouse xenograft model using autocrine lymphocytes also showed that PTPN3 inhibition in LCNEC cells augmented the anti-tumor effect of PTPN3-suppressed activated lymphocytes. In vitro experiments showed that PTPN3 is involved in the induction of malignant traits such as proliferation, invasion and migration. Signaling from PTPN3 is mediated by MAPK and PI3K signals via tyrosine kinase phosphorylation through CACNA1G calcium channel. Our results show that PTPN3 suppression is associated with lymphocyte activation and cancer suppression in lung NET. These results suggest that PTPN3 suppression could be a new method of cancer treatment and a major step in the development of new cancer immunotherapies.

## Introduction

Immune checkpoint inhibitors have recently attracted attention as a new cancer treatment due to their remarkable efficacy [1–3]. We

previously showed that protein tyrosine phosphatase non-receptor type3 (PTPN3), which is upregulated in activated lymphocytes, is a novel immune checkpoint molecule that regulates lymphocyte activation [4]. PTPN3 inhibitors have the potential to be orally administered and

**Abbreviations:** PTPN3, protein tyrosine phosphatase non-receptor type3; PTP, protein tyrosine phosphatase; ERK, extracellular signal-regulated kinase; LCK, lymphocyte-specific protein tyrosine kinase; AKT, protein kinase b; ZAP70, zeta-chain-associated protein kinase 70; GAPDH, glyceraldehyde-3-phosphate dehydrogenase; CDDP, Cis-diamminedichloro-platinum; EGFR, Epidermal growth factor receptor; VEGFA, Vascular endothelial growth factor A; EMT, Epithelial-mesenchymal transition; CACNA1G, Calcium Voltage-Gated Channel Subunit Alpha1 G.

\* Corresponding author

E-mail address: [ohnishi.hideya.928@m.kyushu-u.ac.jp](mailto:ohnishi.hideya.928@m.kyushu-u.ac.jp) (H. Onishi).

<https://doi.org/10.1016/j.tranon.2021.101152>

Received 29 April 2021; Received in revised form 25 May 2021; Accepted 4 June 2021

1936-5233/© 2021 The Authors. Published by Elsevier Inc. This is an open access article under the CC BY-NC-ND license

(<http://creativecommons.org/licenses/by-nc-nd/4.0/>).

appear to be a very promising drug for cancer treatment. However, it is critical to examine how PTPN3 inhibition affects not only lymphocytes, but also cancer.

PTPN3 is one of the 23 isozymes of tyrosine de-phosphatases and dephosphorylates tyrosine residues to negatively regulate certain tyrosine kinase signaling pathways [5]. Upon stimulation of the TCR/CD3 complex in lymphocytes, phosphorylation of Lck and Zap70 is enhanced and the MAPK pathway is activated, resulting in lymphocyte proliferation and hyperfunction. This mechanism increases the expression of PTPN3, which suppresses lymphocyte activation [4]. Several studies have shown that PTPN3 enhances the malignant traits of various cancers. For example, suppressing PTPN3 in non-small cell lung cancer cells led to antitumor effects [6]. Other reports revealed the biological significance of PTPN3 in glioma and ovarian cancer and showed that downregulation of PTPN3 suppressed the malignant traits of glioma and ovarian cancer [7,8]. However, the biological significance of PTPN3 in lung neuroendocrine tumor (NET) including small cell lung cancer (SCLC) and large cell neuroendocrine cancer (LCNEC) has not been examined.

Lung NET is a fast-growing cancer, and chemotherapy and radiation therapy are currently the main treatments for lung NET. Lung NET shows a better response to chemotherapy and radiation therapy than other lung cancers, but its rapid progression and the high incidence of recurrence and metastasis make continuation of chemotherapy and radiation therapy difficult [9]. Therefore, the 5-year survival rate of patients with SCLC and LCNEC is 25% and 32.2%, respectively [10]. Markers such as chromogranin A, pro-gastrin-releasing peptide, and neuron-specific enolase have previously been shown to play important roles in staging and prognosis survival in neuroendocrine tumors [11]. Furthermore, regarding markers, markers for EGFR have been tested in lung cancer and other cancers, and it has been reported that this is also expected to be associated with the development of new therapeutic methods and survival [12]. The development of effective new therapies is critical to improve the treatment and survival of patients with lung NET.

In the present study, we analyzed the biological significance of PTPN3 in lung NET and evaluated the potential of PTPN3 suppression as a treatment for lung NET.

## Materials and methods

### Cell lines

Three human SCLC cell lines, 87–5, SBC5, and S2, were used in this study. The 87–5 and S2 cell lines were purchased from the Cell Resource Center for Biomedical Research Institute of Development, Aging and Cancer Tohoku University, Sendai, Japan. SBC5 cells were obtained from the Japanese Collection of Research Bioresources bank. All cell lines were maintained in RPMI 1640 medium (Nacalai Tesque, Kyoto, Japan) supplemented with 10% fetal calf serum (FCS; Thermo Fisher Scientific, Waltham, MA, USA) and antibiotics (2000 units/ml of penicillin and 10 µg/ml of streptomycin). Cells were cultured at 37 °C in 5% CO<sub>2</sub> and 95% air. The LCNEC cell line generated from a patient with LCNEC at the Fukuoka General Cancer Clinic was used in vivo experiment. This cell line was maintained in DMEM medium (Nacalai Tesque, Kyoto, Japan) supplemented with 10% fetal calf serum.

### Small interfering RNA (siRNA) transfection and lentivirus production

The siRNA targeting PTPN3 (ON-TARGETplus™ SMARTpool, L-009,372) and negative control siRNA (ON-TARGETplus™ Control non-targeting siRNA, D-001,810) were purchased from Dharmacon (Lafayette, CO, USA). Cells ( $0.2 \times 10^6$  cells/well) were seeded in 6-well plates and transfected with siRNA using Lipofectamine RNAiMAX reagent (Invitrogen, Carlsbad, CA, USA) according to the manufacturer's protocol. Cells were used for experiments at 2 days after transfection.

The short hairpin RNA (shRNA) sequence targeting PTPN3 was as follows: GAC AGC TAC TTA GTC TTG ATC CGT A. The oligonucleotides were ligated into a plasmid vector (pcDNA™6.2-GW/EmmiR, #K4934–00; Thermo Fisher Scientific), which was then co-transfected with the ViraPower™ Packaging Mix (included in BLOCK-iT™ Lentiviral Poll I miR RNAi Expression Systems; Thermo Fisher Scientific) into the 293FT cell line to produce lentiviral stock. In experiments using activated lymphocytes, lymphocytes were infected with lentivirus at culture days 3–4.

### Induction of activated lymphocytes

Peripheral blood mononuclear cells (PBMCs) were collected from the heparinized peripheral blood of healthy volunteers and purified using HISTOPAQUE-1077 (Merck KGaA, Darmstadt, Germany) density gradient centrifugation. PBMCs were cultured in RPMI-1640 (Nacalai Tesque) supplemented with 10 µg/ml streptomycin (Meijiseika, Tokyo, Japan), 2000 units/ml penicillin (Meijiseika), 0.5% human serum, and 200 U/ml IL-2 (Primmune, San Diego, CA, USA) in 6-well plates coated with 2.5 µg/ml anti-CD3 monoclonal antibody (OKT3, JANSSEN PHARMACEUTICAL K.K., Osaka, Japan) for 4–7 days. Non-adherent cells were collected as activated lymphocytes.

### DNA microarray

We performed DNA microarray analysis using 87–5 cells as previously described [13]. Intensity-based Z-scores and ratios (non-log-scale fold-change) were calculated from the normalized signal intensities of each probe to compare lymphocytes before and after activation.

### Cell proliferation assay

Cell lines were transfected with PTPN3 siRNA or control siRNA and seeded onto 96-well plates ( $5.0 \times 10^3$  cells/well). Cells were then incubated for 24 and 48 h. Cell proliferation was assessed using Cell Count Reagent SF (Nacalai Tesque, Kyoto, Japan) by measuring absorbance at 492 nm using a plate reader (Biotrak visible plate reader, Amersham Biosciences, Piscataway, NJ, USA) with a reference wavelength of 620 nm.

### Cell invasion assay

The invasive capacity of the SCLC cell lines was assessed by Matrigel invasion assay as described previously [14]. Briefly, siRNA-transfected cells ( $2.0 \times 10^5$ ) were plated in the upper chamber of a Transwell chamber (pore size 8.0 µm; BD Biosciences, Tokyo, Japan) and incubated for 24 h. The cells that migrated to the lower side of the filter were fixed and stained with Diff-Quik reagent (Sysmex, Kobe, Japan) and then counted at 100 × magnification under a light microscope (Nikon Eclipse TE 300, Nikon, Tokyo, Japan).

### Cytotoxicity assay

We modified an adherent target detachment assay described elsewhere [15] to measure the cytotoxicity of activated lymphocytes. Cell lines transfected with PTPN3 siRNA or control siRNA were seeded onto 96-well plates ( $5.0 \times 10^3$  cells/well) and incubated for 24 h to allow adherence. Then, PTPN3 shRNA-expressing lymphocytes ( $1.0 \times 10^6$  cells) was added to one group of PTPN3 siRNA cells and one group of control siRNA cells. Control shRNA-expressing lymphocytes was performed in the same manner, and target and effector cells were co-incubated for 48 h [Effector cells (activated lymphocytes) at an effector/target (E/T) ratio of 20:1 were added to the culture]. Lymphocytes that we used mainly consist of CD3<sup>+</sup> activated T cells [4]. To quantify viable adherent cancer cells, Cell Count Reagent SF was added to the washed wells, followed by incubation for 1 h at 37°C. The

absorbance at 450 nm was then measured using a microplate reader. Viable cancer cells were detected by subtracting the absorbance of lymphocytes alone from that of co-culture. In some cytotoxic assays, siRNA-transfected cells were incubated with or without cisplatin at 0–5 µg/ml for 48 h.

**Reverse transcription (RT)-polymerase chain reaction (PCR)**

Total RNA was extracted using a High Pure RNA Isolation kit (Roche, Basel, Switzerland) and quantified by spectrophotometry (Ultrospec 2100 Pro, Amersham Pharmacia Biotech, Piscataway, NJ, USA). For RT-PCR, 1.0 µg of RNA was reverse transcribed to cDNA with the Verso cDNA Synthesis Kit (Thermo Fisher Scientific) according to the manufacturer’s protocol. RT-PCR reactions were performed using MasterMix kit (Qiagen, Valencia, CA, USA). The primer sets used were as follows: PTPN3 forward, 5'-TGG TAT CGTG GAA GGA CTCA-3'; reverse, 5'-AGC TCC ACCTA GAA GCA CAGAA-3'; and glyceraldehyde- 3-phosphate

dehydrogenase (GAPDH) forward, 5'-CCA CCC ATG GCA AAT TCC ATG GCA -3'; reverse, 5'-TCT AGA CGG CAG GTC AGG TCC ACC-3'.

**Real-time RT-PCR**

RNA (1 µg) was treated with DNase and reverse transcribed using the Quantitect Reverse Transcription kit (Qiagen). Reactions were run on a DNA Engine Opticon 2 System (Bio-Rad, Hercules, CA, USA) using SYBR Premix Ex Taq II (Takara, Otsu, Japan) as previously described [16]. Human PTPN3 primer was purchased from Bio-Rad. The β-actin primer sequences are as follows: forward, 5'-TTG TTA CAG GAA GTC CCT TGCC-3'; reverse, 5'-ATG CTA TCA CCT CCC CTG TGTG- 3'. The amount of each target gene in a given sample was normalized to the level of β-actin mRNA in the sample.

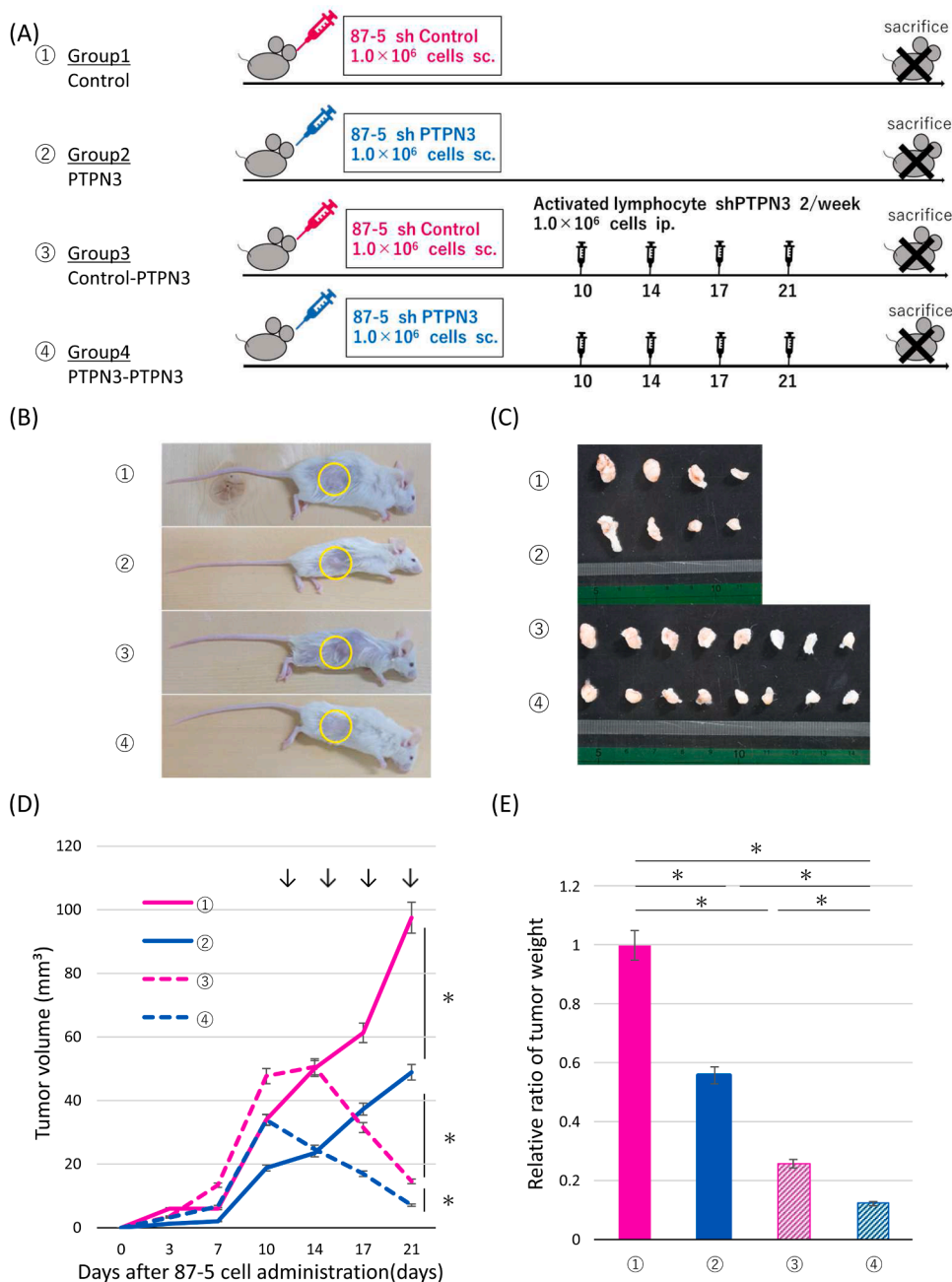


**Fig. 1.** PTPN3 inhibition of SCLC in vivo is enhanced by PTPN3-suppressed activated lymphocytes. (A) NOD-SCID female mice were randomized into four groups (only cells,  $n = 4$ ; cells and lymphocytes,  $n = 8$  per group). Control shRNA or PTPN3 shRNA was introduced into 87-5 cells, and the cells were subcutaneously (sc) transplanted into mice. PTPN3 or control shRNA-infected activated lymphocytes were intraperitoneally (ip) administered on days 10, 14, 17 and 21. Mice were sacrificed and tumors were harvested on day 21. (B) Image of a representative mouse from each group; the tumor is indicated by the yellow circle. (C) Image of tumors from each group. (D) Changes in tumor volume over time. Arrows indicate injections. (E) Tumor weight at 21 days after tumor implantation. Tumor weight was compared. \* $P < 0.05$ . Bar, mean  $\pm$  SD.

### Western blot analysis

Western blotting was performed as described previously [17]. The protein-transferred membranes were incubated overnight at 4 °C with primary antibodies for PTPN3 (1:200, sc-9789; Santa Cruz Biotechnology, Dallas, TX, USA), ERK1/2 (1:1000, No. 9102; Cell Signaling Technology, Danvers, MA, USA), pERK (1:1000, No. 9101; Cell Signaling Technology), Zap (1:2000, No. 3165; Cell Signaling Technology), pZap (1:1000, No. 2701; Cell Signaling Technology), Lck (1:1000, No. 2657; Cell Signaling Technology), pSrc (1:1000, No. 2101; Cell Signaling Technology), Akt (1:1000, sc-8312; Santa Cruz Biotechnology), p-Akt (1:1000, sc-101,629; Santa Cruz Biotechnology), E-cadherin (1:200, sc-7870; Santa Cruz Biotechnology), Vimentin (1:1000, ab92547; Abcam plc), SNAI1 (1:200, sc-271,977; Santa Cruz Biotechnology), Slug (1:200, sc-15,391; Santa Cruz Biotechnology), transforming growth factor- $\beta$ 1 (TGF $\beta$ 1) (1:200, sc-146; Santa Cruz Biotechnology), programmed cell death ligand 1 (PD-L1) (1:400, B7-H1; Biolegend, San Diego, CA, USA), HIF-1 $\alpha$  (1:200, ab5160; Abcam plc), MMP (1:1000, sc-6840; Santa Cruz Biotechnology), EGFR (1:1000, sc-120; Santa Cruz Biotechnology), VEGFA (1:1000, sc-152; Santa Cruz Biotechnology), or CACNA1G (1:1000, ab134269; Abcam plc).

Membranes were then incubated with peroxidase-linked secondary antibodies (Amersham Biosciences) for at least 1 h at room temperature. Immunocomplexes were detected with Amersham ECL Prime Western Blotting Detection Reagent (GE Healthcare, Tokyo, Japan) and visualized with EZ Capture ST (ATTO, Tokyo, Japan). We used  $\alpha$ -Tubulin (1:1000, Sigma-Aldrich, St. Louis, MO, USA) as a protein loading control. Results were quantified using the Image J software program (USA). There is membrane information in the additional file.

### In vivo xenograft tumor model

In Fig. 1, NOD-SCID female mice (4–6 weeks old) were purchased from Charles River Laboratories Japan (Kanagawa, Japan) and acclimated for 2 weeks. All experimental procedures were approved by the Animal Care and Use Committee of Kyushu University (A19–351–0, A19–352–0). All mice were housed and maintained in a specific pathogen-free animal facility at Kyushu University, and all efforts were made to minimize the number of animals used and their suffering. All experiments were performed in strict accordance with the Guidelines for Proper Conduct of Animal Experiments (Science Council of Japan).

NOD-SCID female mice (4–6 weeks old;  $n = 16$ ) were randomized into four groups ( $n = 4$  per group). To establish the model, 87–5 cells transfected with PTPN3 shRNA or control shRNA ( $1.0 \times 10^6$  cells) in 50  $\mu$ l RPMI medium were injected subcutaneously into the bilateral flank of mice (two groups each). Ten days after injection, 50  $\mu$ l of PTPN3 shRNA-expressing lymphocytes ( $1.0 \times 10^6$  cells) was injected into one group of PTPN3 shRNA and one group of control shRNA mice. Lymphocytes were injected intraperitoneally twice per week for 2 weeks (four times total, on days 10, 14, 17 and 21 after cell transplantation). Tumor size was measured twice each week, and tumor volume was calculated as follows:  $A \times B^2 \times 0.5$ , where A is the longest diameter and B is the smaller of the two perpendicular diameters of the tumor. Tumors were measured daily. Animals were monitored for 21 days and then sacrificed on day 21; the tumors were removed for analysis. In Fig. 3, NOD-SCID female mice (4–6 weeks old;  $n = 12$ ) were randomized into three groups ( $n = 4$  per group). As before, LCNEC cell transfected with PTPN3 shRNA or control shRNA ( $1.0 \times 10^6$  cells) in 50  $\mu$ l DMEM medium were injected subcutaneously into the bilateral flank of mice. Lymphocytes were started on day 8 post-injection, which confirmed tumor growth (three times in total, on days 8, 10, and 15 after cell transplantation). Animals were monitored for 17 days and then sacrificed on day 17; the tumors were removed for analysis.

### Immunohistochemistry

Tissue samples were obtained from five patients with SCLC who underwent resection at Japanese Red Cross Fukuoka Hospital, Fukuoka, Japan between 2014 and 2018. Approval for the use of tissues was obtained from patients. Tissue samples obtained from mice implanted with 87–5 cells transfected with PTPN3 siRNA or control siRNA were also analyzed.

Immunohistochemical staining was performed using 4- $\mu$ m-thick formalin-fixed, paraffin-embedded tissue sections and primary antibodies for  $\alpha$ -smooth muscle actin ( $\alpha$ SMA) (1:100, ab5694, Abcam plc, Cambridge, MA, USA), Ki-67 (1:50, sc-15,402, Santa Cruz Biotechnology), vascular endothelial growth factor (VEGF) (1:50, sc-152, Santa Cruz Biotechnology), CD3 (1:100, ab5690, Abcam plc), CD4 (1:100, ab133616, Abcam plc), CD8 (1:50, ab17147, Abcam plc), CD56 (Novocastra, Buffalo Grove, IL, USA), forkhead box P3 (FOXP3) (1:100, ab10563, Abcam plc), PD-L1 (1:100, B7-H1, BioLegend), PTPN3 (PTP-H1) (1:50, sc-515,181, Santa Cruz Biotechnology), or PD-1 (1:100, CD279, BioLegend).

Endogenous peroxidase activity was blocked using 3% hydrogen peroxide solution for 5 min. Antigen retrieval was conducted by a high-pressure method for 10 min with Target Retrieval Solution, pH 9.0 (Agilent Technologies, Santa Clara, CA, USA). The slides were incubated with primary antibodies overnight at 4 °C, followed by incubation for 40 min with secondary antibodies at room temperature. The samples were incubated with HISTOFINE simple stain MAX-PO (R) (Nichirei, Tokyo, Japan) and the labeled antigens were visualized using diaminobenzidine. Counterstaining was performed with hematoxylin. Positive and negative controls were used.

The absolute numbers of labeled tumor-infiltrating cells were manually counted. The total numbers in the ten selected areas were represented as intratumoral CD3-positive T cells, and CD8-positive T cells. For evaluation of  $\alpha$ SMA, Ki-67, PD-L1, PD-1, VEGF, PTPN3, and Masson's Trichrome staining of mouse xenograft tumors, we observed five microscopic fields at 100  $\times$  or 200  $\times$  magnification. Positively stained areas were quantified using Image J software.

PTPN3 expression was evaluated using the Allred score too [18], and  $TS \geq 3$  was used as a cut-off value [19,20] to divide cases into PTPN3 high expression ( $TS \geq 3$ ) and PTPN3 low expression ( $TS < 3$ ) groups.

### Statistical analyses

The data are presented as the mean  $\pm$  standard deviation (SD). Student's t-test was used to compare continuous variables between two groups. p values of  $< 0.05$  were considered statistically significant.

### Results

#### *PTPN3 inhibition in SCLC cells enhances the antitumor effect of PTPN3-suppressed allo activated lymphocytes*

A previous study reported that the cytotoxicity of PTPN3-suppressed activated lymphocytes was significantly enhanced compared with that of control activated lymphocytes [4]. To investigate the potential treatment strategy for PTPN3 inhibition in cancer patients, we performed an experiment using PTPN3-suppressed allo activated lymphocytes and examined the effects on cancer cells with suppression of PTPN3 (Fig. 1A). We randomized NOD-SCID mice into four groups and transplanted 87–5 cells transfected with control shRNA or PTPN3 shRNA (two groups each). On days 10, 14, 17 and 21 after cell transplantation, we then intraperitoneally injected two groups with activated lymphocytes transfected with PTPN3 shRNA; mice group that transplanted 87–5 cells transfected with control shRNA and treated with PTPN3 shRNA-transfected-activated lymphocytes (control-PTPN3 group), and mice group that transplanted 87–5 cells transfected with PTPN3 shRNA and treated with PTPN3 shRNA-transfected-activated

lymphocytes(PTPN3-PTPN3 group). Tumors formed in all mice, and PTPN3 suppression had no effect on the tumor-forming capacity (Fig. 1B, C). In the two groups that did not receive lymphocytes, the tumor volume in the PTPN3 shRNA group was immensely smaller (Fig. 1D) and tumor weight was reduced compared with the control group (Fig. 1E). In the two groups treated with lymphocytes transfected with PTPN3 shRNA, the tumors of the PTPN3 shRNA group were even smaller (Fig. 1D) with reduced weight compared with the control group (Fig. 1E). There were no obvious metastases in any of the mice (data not shown).

*PTPN3 suppression reduces cancer tissue fibrosis and increases the number of infiltrating lymphocytes to the cancer local site*

We next performed immunohistochemical staining of xenograft tumors from each of the four groups. First, we compared control-PTPN3 group and PTPN3-PTPN3 group . We confirmed that PTPN3 was

suppressed in shPTPN3-transfected cancer cells; PD-L1 expression was also decreased and VEGF expression was increased in the tumor tissues of the PTPN3 shRNA group (Fig. 2A). We next examined fibrosis and found that while  $\alpha$ SMA staining showed no difference among groups, Masson Trichrome staining was decreased in the PTPN3 shRNA groups, suggesting that PTPN3 promotes fibrosis. Furthermore, we compared control group and PTPN3 group . Immunostaining confirmed that PTPN3 was suppressed in the cancer cells into which shPTPN3 was introduced and that CD3 and CD8 cells showed increased infiltration into the cancer tissues (Fig. 2B). We compared the infiltration of CD3-positive T cells in the liver and lung and found no difference in the number of infiltrating lymphocytes between the two groups (Additional file1: Fig. S1). We think that administrated activated-lymphocytes moved to the cancer local site in this experiment. These results suggest that PTPN3 inhibition in SCLC cells inhibits cancer tissue fibrosis, enhances lymphocyte infiltration to the cancer local site, and enhances the anti-tumor effects of activated lymphocytes.

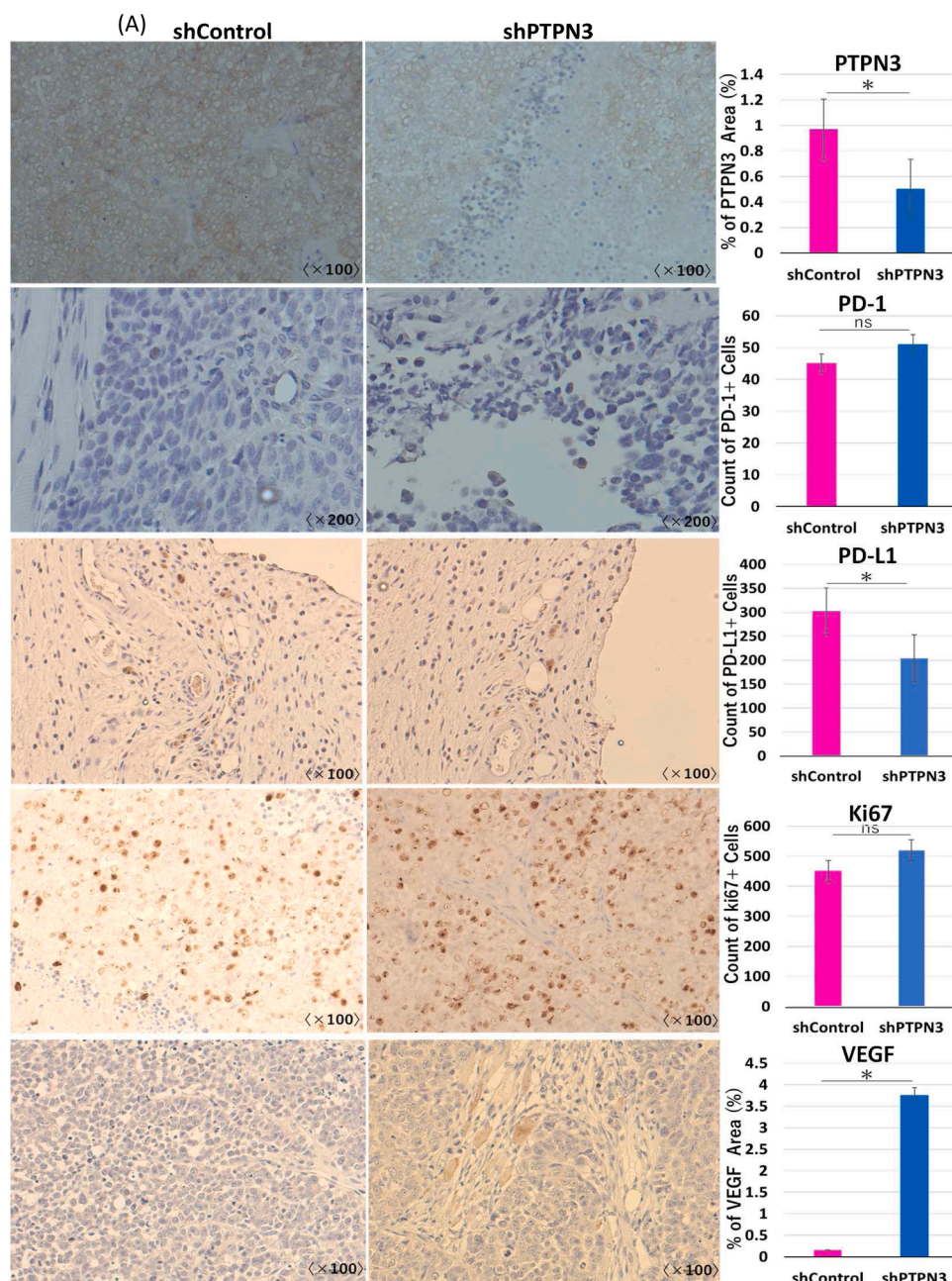


**Fig. 2.** PTPN3 suppression reduces fibrosis of cancer tissue and increases the number of lymphoid cells infiltrating tissue. (A) Representative immunohistochemical staining images of resected xenograft tumors from mice injected with Control shRNA or PTPN3 shRNA cells are shown. (B) Representative immunohistochemical staining images of resected xenograft tumors from mice injected with Control shRNA or PTPN3 shRNA cells are shown. PTPN3, VEGF,  $\alpha$ SMA, Fibrosis (Masson trichrome stain), and CD8 staining: magnification, 100x. Ki67, PD-1, PD-L1, and CD3 staining: magnification, 200x. \* $P < 0.05$ . Bar, mean  $\pm$  SD; n.s., not significant.

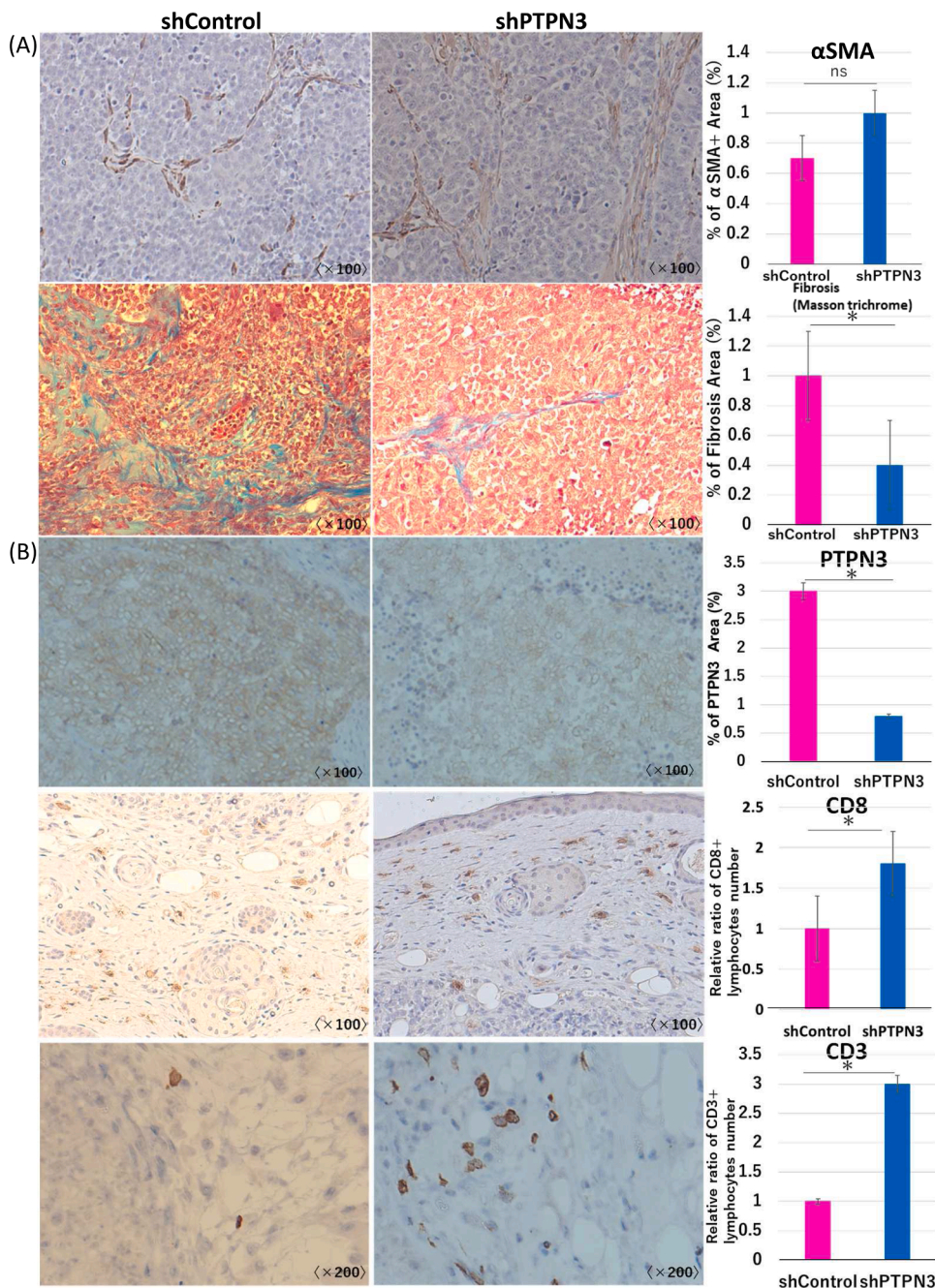


Fig. 2. (continued).

*PTPN3 inhibition in LCNEC cells enhances the antitumor effect of PTPN3-suppressed autocrine activated lymphocytes*

To confirm the therapeutical effect of PTPN3 inhibition the experiment that used LCNEC cells and autologous lymphocytes from same patient with LCNEC was performed (Fig. 3A). To start the experiment, we confirmed Western blot analysis showed that PTPN3 was expressed in LCNEC cell line (Fig. 3B). In this experiment we randomized NOD-SCID mice into three groups: mice group that transplanted LCNEC cells transfected with control shRNA and treated with control shRNA-transfected-activated lymphocytes (control-control group), mice group that transplanted LCNEC cells transfected with control shRNA and treated with PTPN3 shRNA-transfected-activated lymphocytes (control-PTPN3 group), and mice group that transplanted LCNEC cells transfected with PTPN3 shRNA and treated with PTPN3 shRNA-transfected-activated lymphocytes (PTPN3-PTPN3 group). On days 8, 10 and 15

after cell transplantation, we then intraperitoneally injected three groups with activated lymphocytes. Firstly, considering the systemic therapy with PTPN3 inhibition, control-control group and PTPN3-PTPN3 group were compared. Tumors formed in all mice (Fig. 3C) and the tumor volume in the PTPN3-PTPN3 group was significantly smaller than that in control-control group (Fig. 3D). When three group were compared, the tumor volume in the control-PTPN3 group was significantly smaller than that in control-control group and larger than that in the PTPN3-PTPN3 group (Fig. 3D). Tumor weight was significantly reduced compared with the control group (Fig. 3E).

We next examined the infiltrated lymphocytes into cancer cells by immunostaining and revealed that CD3 and CD8 cells showed increased infiltration into the cancer tissues in the PTPN3-PTPN3 group compared with control-control group (Fig. 3F,G).

These results suggest that a PTPN3 inhibition could be a new cancer treatment with a dual effect of LCNEC lymphocyte activation and cancer

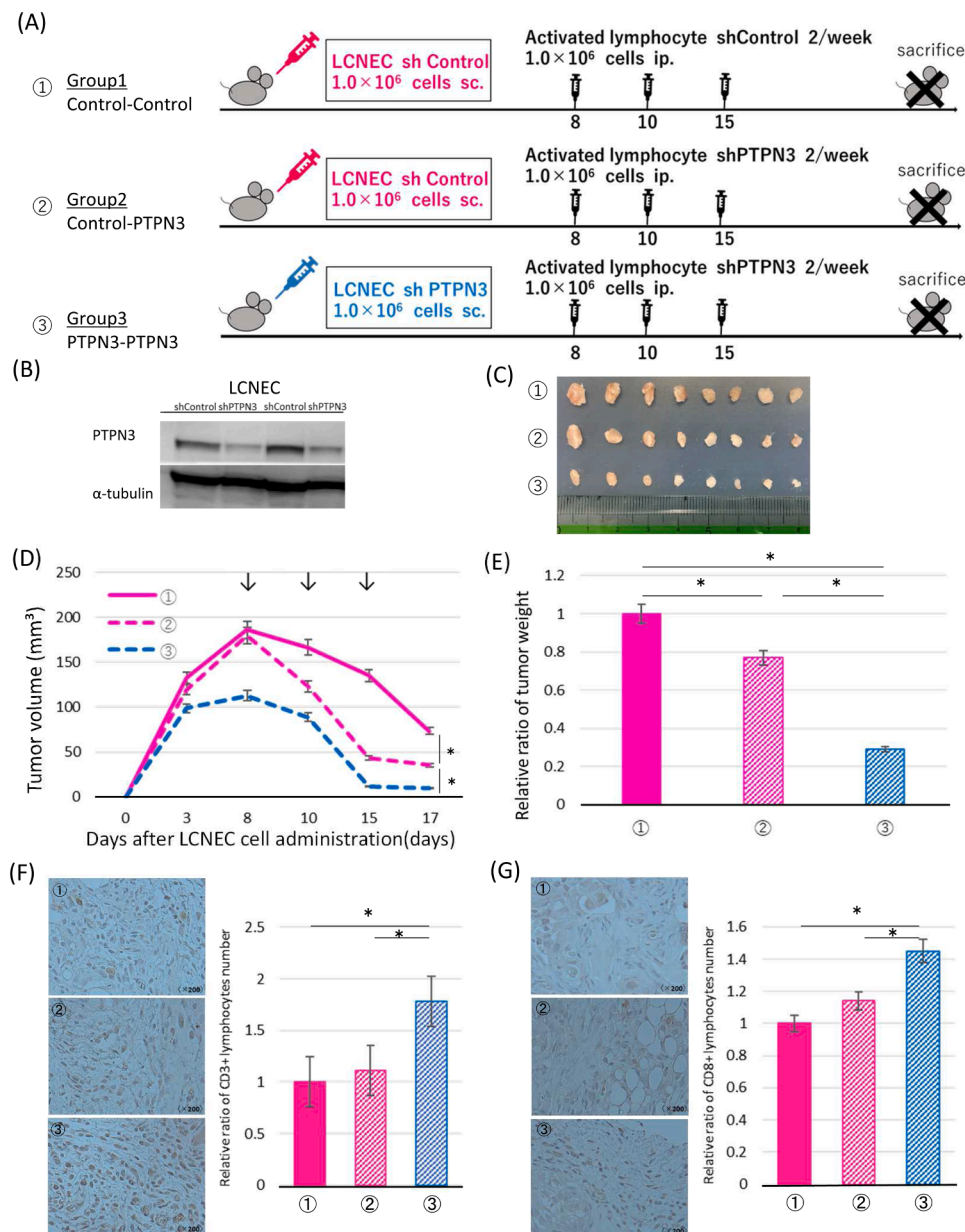


**Fig. 3.** Cancer cells and autologous lymphocytes from LCNEC patients were used for treatment experiments in mice. (A) Western blot analysis of LCNEC cell line transfected with PTPN3 or control siRNA. (B) NOD-SCID female mice were randomized into three groups ( $n = 8$  per group). Control shRNA or PTPN3 shRNA was introduced into LCNEC cells, and the cells were subcutaneously (sc) transplanted into mice. PTPN3 or control shRNA-infected activated lymphocytes were intraperitoneally (ip) administered on days 8, 10 and 15. Mice were sacrificed and tumors were harvested on day 17. (C) Image of tumors from each group. (D) Changes in tumor volume over time. Arrows indicate injections. (E) Tumor weight at 17 days after tumor implantation. Tumor weight was compared. (F,G) Representative immunohistochemical staining images of resected xenograft tumors from mice injected with Control shRNA or PTPN3 shRNA cells are shown. CD8 and CD3 staining; magnification, 200x. \* $P < 0.05$ . Bar, mean  $\pm$  SD.

**Table 1**

Characteristics of the five clinical SCLC cases.

M: Male; F: Female; RUL: Right Upper Lobe; RML: Right Middle Lobe; RLL: Right Lower Lobe.

	Case1	Case2	Case3	Case4	Case5
Age(years)	80	66	76	76	60
Gender	M	M	F	M	M
Symptoms	(+)	(-)	(-)	(-)	(-)
Tumor location	RUL	RUL	RML	RLL	RLL
Surgical procedure	Lobectomy	Lobectomy	Lobectomy	Lobectomy	Pneumectomy
Tumor size(mm)	16 $\times$ 13	33 $\times$ 22	22 $\times$ 21	35 $\times$ 20	19 $\times$ 12
UICC T category	T1b	T2a	T2a	T2a	T1a
UICC N category	N0	N0	N0	N0	N1
Pleural invasion	PL0	PL0	PL3	PL2	PL0
Lymphatic permeation	Ly0	Ly0	Ly1	Ly0	Ly1
Venous invasion	V0	V1	V1	V0	V0
Bronchial transection	(-)	(-)	(-)	(-)	(-)
Stage classification	IA	IB	IB	IB	IA
Postoperative chemotherapy	(-)	(+)	(-)	(+)	(+)
Recurrence	(-)	(+)	(-)	(+)	(+)
Survival	(+)	(+)	(+)	(+)	(-)
Overall survival(months)	23	51	31	19	63

suppression even in autocrine setting.

*PTPN3 could be involved in increased cancer tissue fibrosis, decreased CD8/FOXP3 ratio and suppressed cellular immunity*

Next, we analyzed five surgically resected SCLC cases to investigate the potential association between PTPN3 expression and clinicopathological or cancer microenvironment-related factors. The characteristics of the five cases are shown in Table 1. Immunostaining of the resected tissues was performed and PTPN3, CD8, Foxp3,  $\alpha$ SMA and Masson's Trichrome staining was evaluated (Fig. 4A). Masson's Trichrome staining revealed a tendency for increased fibrosis in tumor tissues with high expression of PTPN3. Together these results suggest that PTPN3 could be involved in the fibrosis of cancer tissues and reduction of the tissue-infiltrating CD8/FOXP3 ratio, and that patients with high PTPN3 expression may have suppressed cellular immunity. The ratio of the number of CD8 -positive lymphocytes infiltrating the tissue to the

number of regulatory T cells (Treg cells) that negatively regulate immunity is often used as an indicator of cellular immunity [21]. Treg cells suppress the immune response and regulate development, differentiation, and immunosuppressive function via the activity of Foxp3. PTPN3 expression was evaluated using the Allred score. Total score (TS)  $\geq 3$  was used as a cut-off value to divide cases into two groups: PTPN3 high expression, with TS  $\geq 3$ , and PTPN3 low expression, with TS  $< 3$ . The ratio of CD8-positive cells to FOXP3-positive cells was compared between the two groups (Fig. 4B). The CD8/FOXP3 cell ratio was immensely higher in the PTPN3 low expression group than in the PTPN3 high expression group. These results were consistent with the xenograft studies, suggesting that PTPN3 may be involved in fibrosis and cell-mediated immunity.

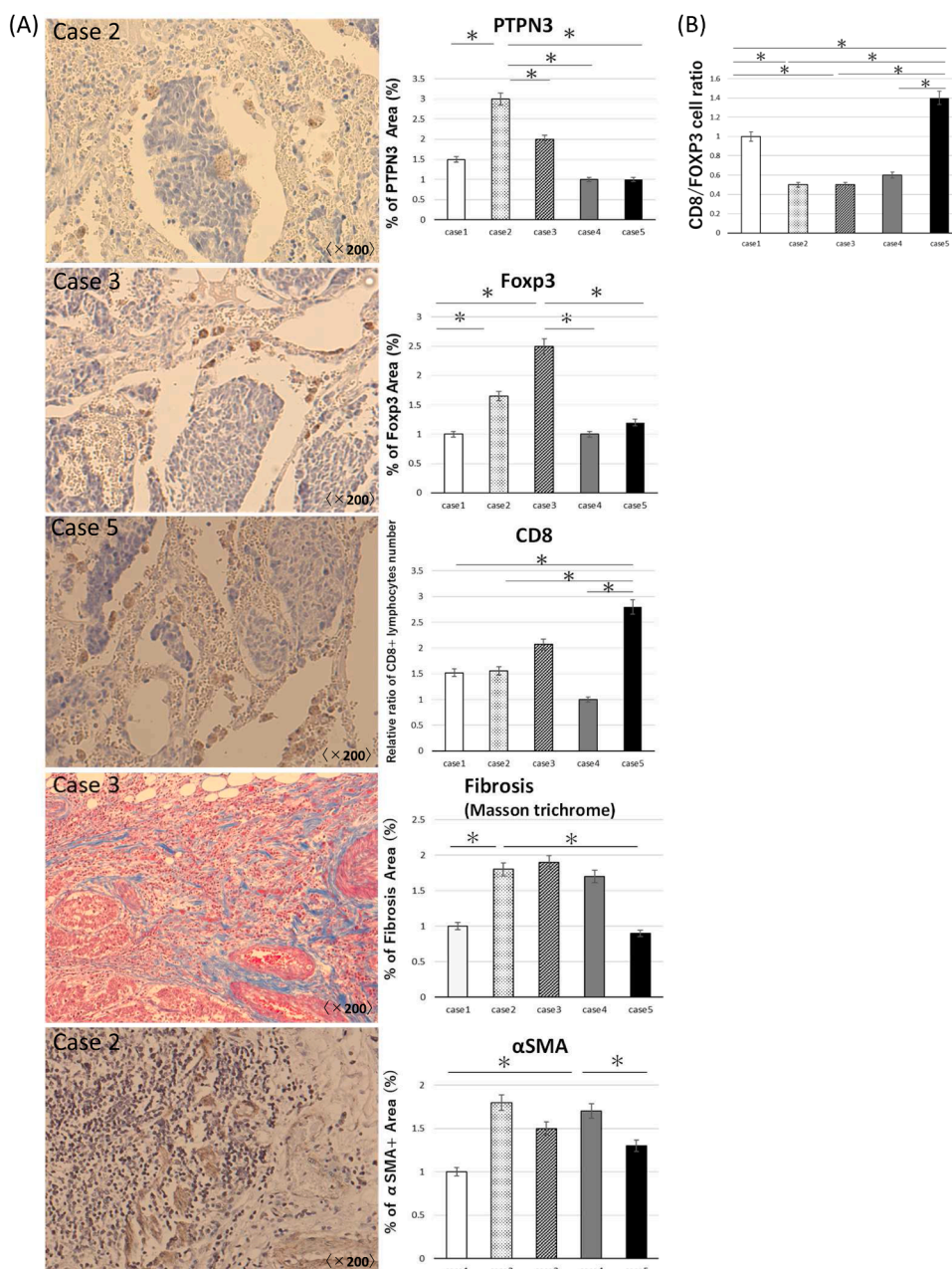


**Fig. 4.** Immunohistochemical staining analysis in clinical case specimens of SCLC. (A) Representative immunohistochemical staining of tumors from patients with SCLC for CD8, Foxp3, PTPN3,  $\alpha$ SMA, and Fibrosis (Masson trichrome staining) (top to bottom) are shown on the left (magnification 200x). Graphs quantifying the numbers of positively stained cells in the five SCLC cases are shown on the right. (B) Ratio of tumor-infiltrating CD8/Foxp3-positive cells in the five SCLC cases are shown on the right. \* $P < 0.05$ . Bar, mean  $\pm$  SD.



*PTPN3 is involved in malignant traits of SCLC, including proliferation, migration, invasion and endothelial-mesenchymal transition (EMT)*

The above results in mice and excised tissues suggested that PTPN3 induces malignant traits in SCLC. Therefore, we next analyzed the effects of PTPN3 on cancer cell proliferation, migration, and invasion in vitro using three SCLC cell lines (87-5, SBC5 and S2) transfected with PTPN3 or control siRNA. We found that proliferation was immensely reduced in 87-5 and SBC5 cells with PTPN3 knockdown, while it was significantly enhanced in S2 cells with PTPN3 knockdown (Fig. 5A). Invasion and migration were also significantly reduced in 87-5 and SBC5 cells with PTPN3 knockdown, but significantly increased in S2 cells with PTPN3 knockdown (Fig. 5B, C). PTPN3 knockdown did not impact cisplatin-induced cytotoxicity in all cell lines (Fig. 5D). These results suggest that PTPN3 is involved in the induction of malignant cancer traits such as proliferation, migration, and invasion in 87-5 and SBC5 cells, while PTPN3 is involved in the suppression of malignant cancer traits in S2 cells.

To confirm the results from the experiments in mice (Fig. 1), we also conducted experiments on cancer cell injury by co-culturing cancer cells transfected with PTPN3 or control siRNA with activated lymphocytes transfected with control shRNA and PTPN3 shRNA. In all three cell lines, the highest cytotoxicity was observed in the co-culture of cancer cells transfected with PTPN3 siRNA plus lymphocytes expressing PTPN3 shRNA (Fig. 5E).

Western blot analysis showed that PTPN3 was highly expressed in all three SCLC cell lines (Fig. 5F). Suppression of PTPN3 expression promoted expression of the EMT-related molecule E-cadherin and increased vimentin in the 87-5 and SBC5 cell lines; conversely, E-cadherin was reduced and vimentin expression was increased in the S2 cell line. Both TGF- $\beta$  and MMP were unchanged in all three cell lines in response to PTPN3 knockdown. These results suggested that PTPN3 is involved in infiltration ability and proliferation ability through EMT [22,23].

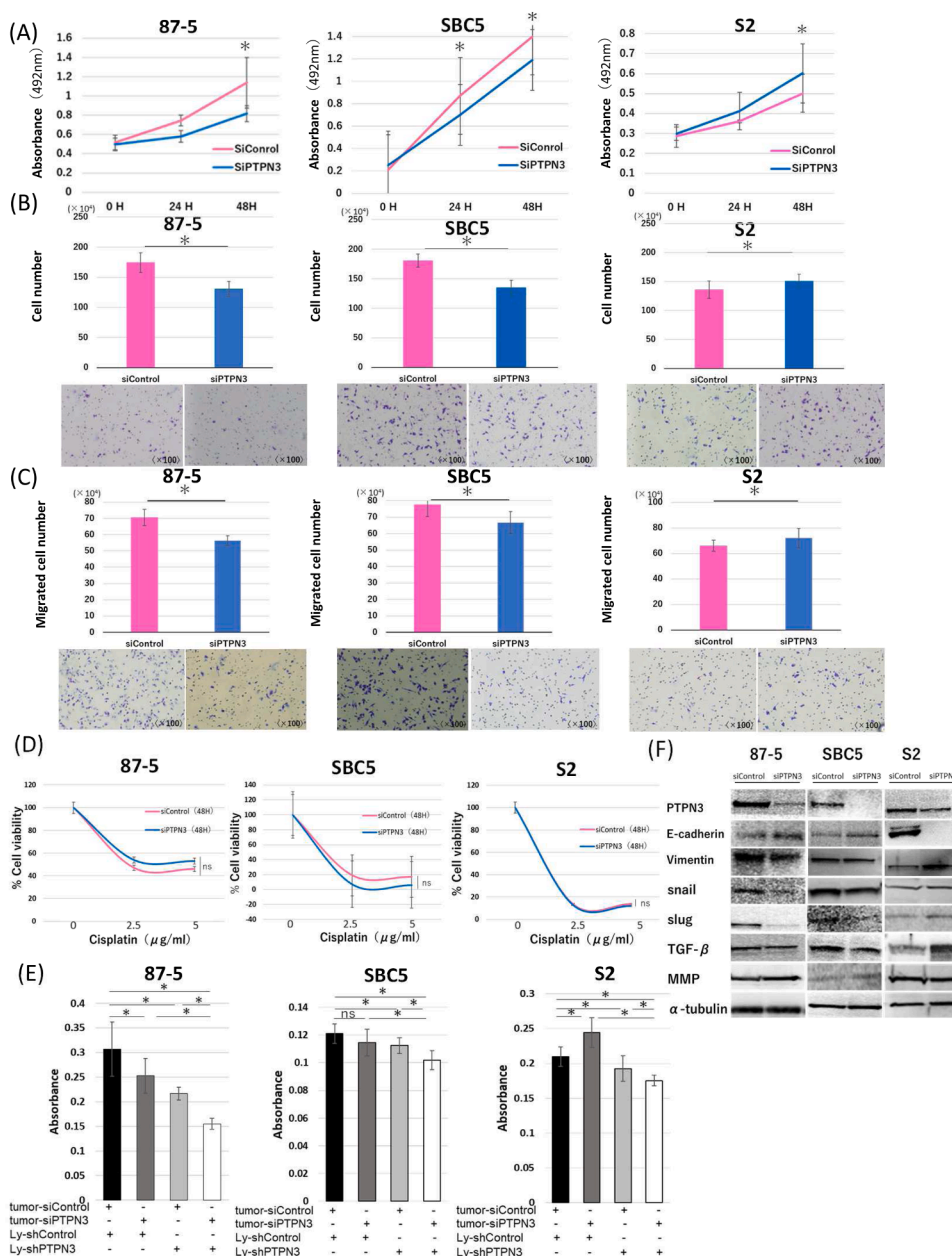


**Fig. 5.** PTPN3 plays a role in SCLC cell proliferation, migration and invasion. SCLC cell lines were transfected with PTPN3 or control siRNA and evaluated for (A) proliferative capacity, (B) invasion capacity, and (C) migratory capacity afterwards. (D) To determine cell response to cisplatin (CDDP), cells were transfected with the indicated siRNAs and treated with 0, 2.5, or 5  $\mu\text{g/ml}$  for 48 h. (E) A cancer cell injury experiment was performed by co-culturing cancer cells transfected with Control siRNA or PTPN3 siRNA (Csi or Psi, respectively) with activated lymphocytes expressing Control shRNA or PTPN3 shRNA (shC or shP, respectively). (F) Western blot analysis of SCLC cell lines transfected with PTPN3 or control siRNA. \* $P < 0.05$ . Bar, mean  $\pm$  SD; n.s., not significant.

### Signals from PTPN3 went through MAPK and PI3K signaling via tyrosine kinase phosphorylation

Since PTPN3 functions by reversing tyrosine kinase-mediated phosphorylation, we next analyzed tyrosine kinase phosphorylation and the downstream signals. In activated lymphocytes, Lck and Zap70 phosphorylation increases and the tyrosine kinase MAPK pathway is induced. The enhanced levels of pZAP70 and pSrc lead to increased expression of PTPN3. When PTPN3 was suppressed in 87-5 and SBC5 cells, pZap70 and pSrc expression were suppressed, and pERK and pAkt levels were also reduced. This suggests that the signal from PTPN3 passes through the MAPK pathway and PI3K/Akt pathway (Fig. 6A). Consistent with our previous experiments in the three SCLC cell lines, we observed opposite results in S2 cells, in which PTPN3 suppression resulted in increased pZap70 and pSrc levels and pERK and pAkt were also elevated compared with controls.

To comprehensively analyze the genes altered by PTPN3, we also performed microarray analysis of 87-5 and SBC5 cells transfected with PTPN3 or control siRNAs (Additional file2: Fig. S2). The results of 87-5 indicated that EGFR and VEGFA gene expressions were highly upregulated in response to PTPN3 knockdown (Additional file3: Fig. S3).

Consistent with these findings, we found that the protein expressions of EGFR was upregulated in 87-5 and SBC5 cell lines transfected with PTPN3 siRNA, while downregulated expression was observed in S2 cells. In addition to this, the protein expressions of VEGFA was upregulated in 87-5 cell lines transfected with PTPN3 siRNA (Fig. 6B). A previous study showed that VEGF expression and HIF-1 $\alpha$  expression are significantly correlated [24]. However, HIF-1 $\alpha$  showed no change in expression in response to PTPN3 knockdown. In the analysis of tyrosine kinase activation correlated with PTPN3 by microarray analysis, expression of Calcium Voltage-Gated Channel Subunit Alpha1 G (CACNA1G) gene that regulates calcium channel was decreased in 2 cell lines transfected with PTPN3 siRNA (Additional file3). Protein expression of CACNA1G in PTPN3-inhibited 87-5, SBC5, and S2 cells was decreased compared to control (Fig. 6C). These results suggest that PTPN3 may activate CACNA1G calcium channel and it results in tyrosine kinase activation.

### Discussion

We previously showed that PTPN3 plays a pivotal role as an immune-checkpoint in activated lymphocytes [4]. Therefore, to explore the potential of PTPN3-targeting systemic treatment, we assessed the

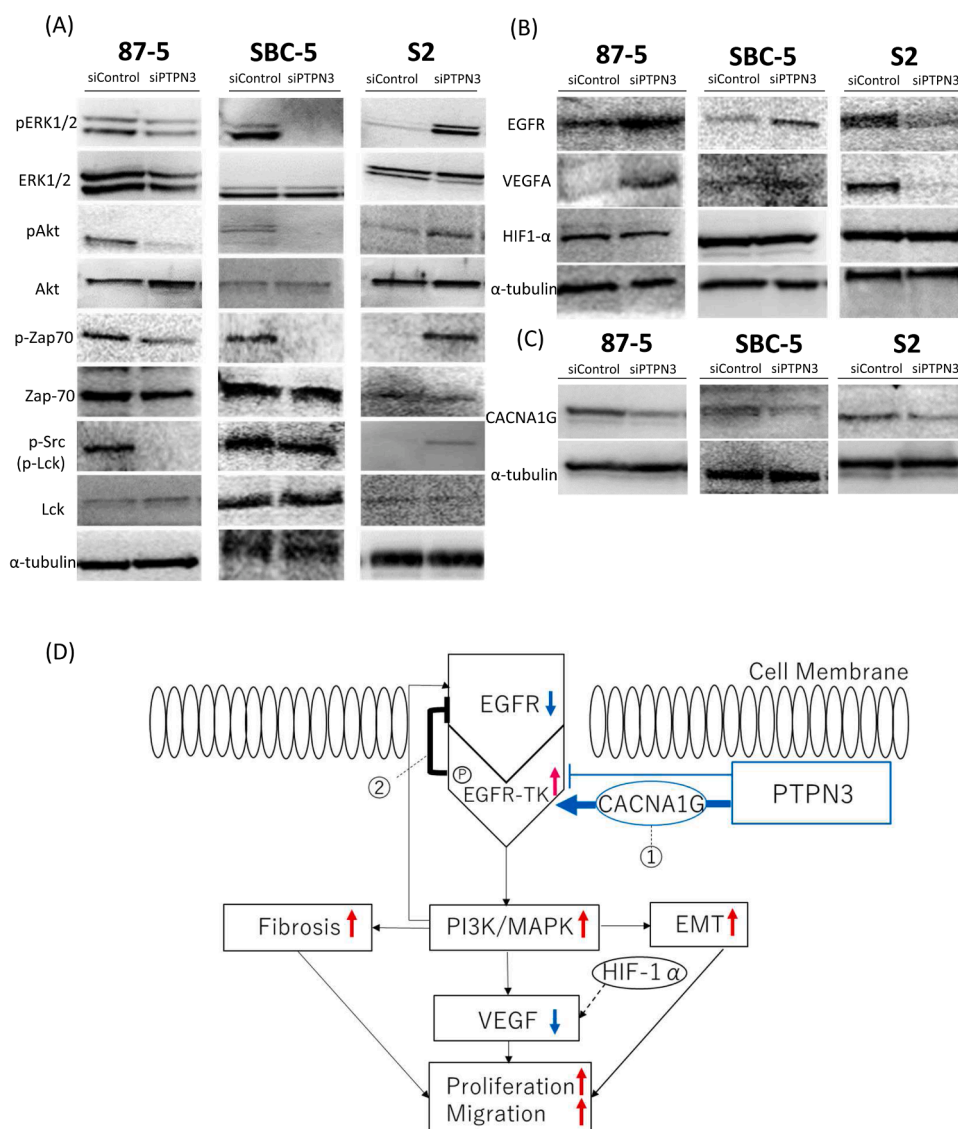


**Fig. 6.** Signal from PTPN3 passes through the MAPK pathway and the PI3K/Akt pathway via tyrosine kinase phosphorylation. (A, B, C) Western blot analysis of SCLC cell lines transfected with PTPN3 or control siRNA. (D) Schematic model summarizing the results of this study. Bold lines are new findings, and dotted line is not relevant this time. Our findings suggest that suppression of PTPN3 reduces proliferation, fibrosis, and EMT in some SCLCs.

biological significance of PTPN3 in cancer cells in the presence of PTPN3-suppressed allo or autocrine activated lymphocytes (Fig. 1 and 3). The results showed that PTPN3-targeting therapy in both lymphocytes and tumor cells was more effective in preventing lung NET growth, indicating the efficacy of PTPN3 suppression in systemic treatment for lung NET.

In this study, we examined the potential associations between PTPN3 expression and clinicopathological factors in SCLC clinical cases. Our study included a limited number of cases as because of the paucity of symptoms and rapid progression of SCLC, and therefore few cases are indicated for surgery at the time of diagnosis. However, lower PTPN3 expression tended to associate with decreased tissue fibrosis, increased tissue-infiltrating lymphocytes and decreased Treg cell infiltration. These results are consistent with the experiments in mice, suggesting the efficacy of PTPN3 inhibition therapy for SCLC.

Although the direct effect of PTPN3 on the linkage between cancer fibrosis and CD8-positive T cell infiltration remains unclear, previous studies reported that protein tyrosine kinase (PTK) induces fibrosis in some diseases [25] and regulates fibrosis through tyrosine kinase inhibition [26]. PTPs regulate tyrosine phosphorylation in concert with PTK [27]. Low expression of PTPN3, like PTK, may lead to reduction of fibrosis because of the interaction between PTK and PTP, which makes it easier for tumor-infiltrating lymphocytes to infiltrate and increase in tissues [28]. Various factors have been reported to be involved in fibrosis. In the liver, activation of hepatic stellate cells can produce fibrosis-inducing factors such as TGF- $\beta$ , and VEGF can activate receptor tyrosine kinases via the VEGF receptor to cause fibrosis [15]. In SCLC, factors within the tumor may also influence the expression of PTPN3 and fibrosis-inducing factors.

We examined the impact of PTPN3 expression on sensitivity to cisplatin in SCLC, but there was no correlation between PTPN3 expression and susceptibility to cisplatin. We speculate this result may be because all cases were previously treated with cisplatin. Notably, only a few PTPN3-positive lymphocytes were detected in SCLC specimens. PCR results revealed seven-fold higher PTPN3 mRNA expression in 87–5 cancer cells than in lymphocytes (Additional file4: Figure S4), suggesting that PTPN3 expressed in lymphocytes may be masked in analyses focusing on PTPN3 expressed in cancer.

Our western blot analysis showed that in SCLC cells with PTPN3 knockdown, pathways involved in cancer progression, such as VEGF signaling and EMT induction, were induced. VEGF is well known as a downstream factor of HIF-1 $\alpha$ . In PTPN3 knockdown cells, an increase in VEGF was observed, but HIF-1 $\alpha$  level was unchanged. These results suggest a specific induction pathway for PTPN3 to promote VEGF elevation independent of HIF-1 $\alpha$ .

A schematic model summarizing the results of our study is shown in Fig. 6D. Our findings suggest that PTPN3 is involved in regulating proliferation, invasion, fibrosis, and EMT in some SCLCs. We previous showed that inhibition of PTPN3 activated lymphocytes through inducing increased phosphorylation of ZAP70, LCK and ERK1/2 [4]. However, in the present study, we found that PTPN3 downregulation suppressed p-Zap70 and p-Src levels in two of the three cancer cell lines, while opposite effects were observed in the third cell line. In the two cancer cell lines in which PTPN3 augments p-Zap70 and p-Src levels, we speculate that a mutation causes a process in which PTPN3 enhances tyrosine kinase phosphorylation, which may surpass the original action of tyrosine kinase dephosphorylation of PTPN3 (hypothesis ①). We think that one of its candidate may be a CACNA1G activation because CACNA1G is reported to contribute to protein kinase phosphorylation [29]. Furthermore, a negative feedback effect on EGFR expression may have been triggered; as a result of the increase in EGFR-TK due to PTPN3, there is a possibility that the expression of EGFR may be increased in cancer cells (hypothesis ②) [30]. Therefore, lung NETs with high expression of PTPN3 have reduced EGFR expression, and anti EGFR mAb agents, which are effective in lung adenocarcinoma, may be ineffective.

Similar to our results showing that PTPN3 has an inhibitory effect on activation in lymphocytes [4], PTPN3 has been reported to suppress malignant traits in NSCLC [6]. In one of the three cancer cell lines we used in this study, PTPN3 acted in the same way as in NSCLC cells, and in such carcinomas, PTPN3 suppression would result in activating the cancer. With respect to the chemotherapy, in some cases of adenocarcinoma, which is NSCLC, tyrosine kinase inhibitors are effective. Although the effects of tyrosine kinase inhibitors in SCLC are unknown [31], the cell line-specific role of PTPN3 in SCLC may have significant implications for the response to chemotherapy in SCLC. Further mechanism analysis of PTPN3 for SCLC cell lines is needed.

Lymphocytes that we used mainly consist of CD3<sup>+</sup> T cells but not NK cells [4]. On the other hand, we performed the experiment using allo activated T lymphocytes in addition to the experiment using autocrine activated T lymphocytes. Regarding the cytotoxicity of lymphocytes, we think that FAS/FAS ligand interaction or MICA/NGK2D interaction may contribute in the experiment using allo activated lymphocytes. Effects of TNF- $\alpha$  as a single cytotoxic mediator against K-562 cells was examined by LDH release and compared with NK cell cytotoxicity [32]. It is useful as a very simple and quick test. However, in our experiment, several cytotoxic mediators may affect the cytotoxicity and we used the methodology of the quantification of the viable cancer cells.

PTPN11 has been reported to be a major mediator of programmed cell death protein-1 (PD-1) and immune checkpoint pathways that negatively regulate B and T lymphocytes [33–35]. In cancer cells, when PD-1 is phosphorylated, it binds to the SHp domain in SHp-2 (PTPN11), which causes T cell activation [36]. Interestingly, PTPN3 is the only PTPN that is upregulated in activated lymphocytes, and PTPN11 is not involved [4]. In this respect, PTPN3 inhibitor therapy may have a different mechanism of action than anti-PD-1 antibody drugs and may be a new addition to existing therapies. PTPs may receive more attention as potential cancer therapeutics in the future.

## Conclusions

In this study, we found that suppressing PTPN3 in some SCLCs and LCNEC yields a cancer-suppressing effect. Our results indicate that PTPN3 inhibitor therapy may be a powerful tool for the activation of lymphocytes in refractory lung NET and inhibition of cancer progression. A PTPN3 inhibitor could be a new cancer treatment with a dual effect of Intractable lung NET lymphocyte activation and cancer suppression. The results of this study may prove significant for the development of new cancer immunotherapies for lung NET.

## Declaration of Competing Interest

The authors declare that they have no conflicts of interest.

## Ethics approval and consent to participate

All procedures involving human participants were in accordance with the ethical standards of the Kyushu University Ethics Committee (study approval number 30–230) and with the 1964 Helsinki declaration and its later amendments or comparable ethical standards. All procedures involving animals were in accordance with the ethical standards of the Animal Care and Use Committee of Kyushu University (study approval numbers A19–351–0 and A19–352–0).

## Consent for publication

Written informed consent was obtained before blood collection from all participants included in the study for the use of PBMCs and tumor specimens for research and publication.

### Availability of data and materials

Data sharing not applicable as no datasets generated and/or analyzed for this study. All data relevant to the study are included in the article or uploaded as supplementary information.

### Funding

This study was supported by the Japan Society for the Promotion of Science (KAKENHI Grant Number JP19K 09124, JP 19 K 09047, and JP 20 K 09180).

### Acknowledgments

We thank Ms. Emi Onishi for her skillful technical assistance and Gabrielle White Wolf, PhD, from Edanz Group (<https://en-author-services.edanzgroup.com/ac>) for editing a draft of this manuscript.

### Author contributions

Conception and design: S.K., H.O. and M.N.; Data acquisition and analysis: S.K., K.N., A.I., S.M., A.F., K.N. and M.K.; writing and original draft preparation: S.K. and S.I.; critical review and editing: S.K., K.M., M. U., T.M., M.N. and H.O.; supervision: H.O. and M.N.; funding acquisition: K.N. and H.O. All authors have seen the final draft of the manuscript before submission.

### Supplementary materials

Supplementary material associated with this article can be found, in the online version, at [doi:10.1016/j.tranon.2021.101152](https://doi.org/10.1016/j.tranon.2021.101152).

### References

- [1] Y. Ishida, Y. Agata, K. Shibahara, et al., Induced expression of PD-1, a novel member of the immunoglobulin gene superfamily, upon programmed cell death, *EMBO J.* 11 (1992) 3887–3895.
- [2] D.R. Leach, M.F. Krummel, J.P. Allison, et al., Enhancement of antitumor immunity by CTLA-4 blockade, *Science* 271 (1996) 1734–1736.
- [3] J. Brahmer, K.L. Reckamp, P. Baas, et al., Nivolumab versus docetaxel in advanced squamous-cell non-small-cell lung cancer, *N. Eng. J. Med.* 373 (2015) 123–135.
- [4] A. Fujimura, K. Nakayama, A. Imaizumi, et al., PTPN3 expressed in activated T lymphocytes is a candidate for a non-antibody-type immune checkpoint inhibitor, *Cancer Immunol. Immunother.* 68 (2019) 1649–1660.
- [5] S. Han, S. Williams, T. Mustelin, Cytoskeletal protein tyrosine phosphatase PTPH1 reduces T cell antigen receptor signaling, *Eur. J. Immunol.* 30 (2000) 1318–1325.
- [6] M.Y. Li, P.L. Lai, Y.T. Chou, et al., Protein tyrosine phosphatase PTPN3 inhibits lung cancer cell proliferation and migration by promoting EGFR endocytic degradation, *Oncogene* 34 (2015) 3791–3803.
- [7] Z.H. Shi, X.G. Li, W.D. Jie, et al., PTPH1 promotes tumor growth and metastasis in human glioma, *Eur. Rev. Med. Pharmacol. Sci.* 20 (2016) 3777–3787.
- [8] S. Li, J. Cao, W. Zhang, et al., Protein tyrosine phosphatase PTPN3 promotes drug resistance and stem cell-like characteristics in ovarian cancer, *Sci. Rep.* 6 (2016) 36873.
- [9] J. Li, C.H. Dai, P. Chen, et al., Survival and prognostic factors in small cell lung cancer, *Med. Oncol.* 27 (2010) 73–81.
- [10] Ke Han1, Haitang Yang, Liwen Fan, et al., Outcomes of patients with large cell neuroendocrine carcinoma of the lung after complete resection, *Transl. Cancer Res.* 6 (3) (2017) 483–492.
- [11] P. Marina, B. Zoran, Z. Vladimir, et al., The prognostic significance of circulating neuroendocrine markers chromogranin A, pro-gastrin-releasing peptide, and neuron-specific enolase in patients with small-cell lung cancer, *Med. Oncol.* (2) (2014) 823.
- [12] J. Vladimir, V. Vladimir, O. Jasmina, et al., EGFR polymorphism and survival of NSCLC patients treated with TKIs: a systematic review and meta-analysis, *J. Oncol.* 2020 (2020), 1973241.
- [13] E. Miyahara, T. Nishikawa, T. Takeuchi, et al., Effect of myeloperoxidase inhibition on gene expression profiles in HL-60 cells exposed to 1, 2, 4, 6-benzenetriol, *Toxicology* 317 (2014) 50–57.
- [14] S. Matsushita, H. Onishi, K. Nakano, et al., Hedgehog signaling pathway is a potential therapeutic target for gallbladder cancer, *Cancer Sci.* 105 (2014) 272–280.
- [15] T. Tsuchida, S.L. Friedman, Mechanisms of hepatic stellate cell activation, *Nat. Rev. Gastroenterol. Hepatol.* 14 (2017) 397–411.
- [16] T. Ogino, H. Onishi, H. Suzuki, et al., Inclusive estimation of complex antigen presentation functions of monocyte-derived dendritic cells differentiated under normoxia and hypoxia conditions, *Cancer Immunol. Immunother.* 61 (2012) 409–424.
- [17] K. Suyama, H. Onishi, A. Imaizumi, et al., CD24 suppresses malignant phenotype by downregulation of SHH transcription through STAT1 inhibition in breast cancer cells, *Cancer Lett.* 374 (2016) 44–53.
- [18] D.C. Allred, J.M. Harvey, M. Berardo, et al., Prognostic and predictive factors in breast cancer by immunohistochemical analysis, *Mod Pathol.* 11 (1998) 155–168.
- [19] Harvey J.M., Clark G.M., Osborne C.K., et al. Estrogen receptor status by immunohistochemistry is superior to the ligand-binding assay for predicting response to adjuvant endocrine therapy in breast cancer. *J Clin Oncol*199;17: 1474–81.
- [20] S.K. Mohsin, H. Weiss, T. Havighurst, et al., Progesterone receptor by immunohistochemistry and clinical outcome in breast cancer: a validation study, *Mod. Pathol.* 17 (2004) 1545–1554.
- [21] E. Shinto, K. Hase, Y. Hashiguchi, et al., CD8+ and FOXP3+ tumor-infiltrating T cells before and after chemoradiotherapy for rectal cancer, *Ann. Surg. Oncol.* 21 (2014) 414–421.
- [22] W. Lingli, W. Ruirui, Y. Zi, et al., PVT1 affects EMT and cell proliferation and migration via regulating p21 in triple-negative breast cancer cells cultured with mature adipogenic medium, *ABBS* 50 (2018) 1211–1218.
- [23] H. Min, W. Ya-Peng, Z. Ling-Qin, et al., MAPK pathway mediates epithelial-mesenchymal transition induced by paraquat in alveolar epithelial cells, *Environ. Toxicol.* 31 (2016) 1407–1414.
- [24] L. Mizokami, K. Kakeji, Y. Oda, et al., Clinicopathologic significance of hypoxia-inducible factor 1 alpha overexpression in gastric carcinomas, *J. Surg. Oncol.* 94 (2006) 149–154.
- [25] E.J. Baxter, L.M. Scott, P.J. Campbell, et al., Acquired mutation of the tyrosine kinase JAK2 in human myeloproliferative disorders, *Lancet* 365 (2005) 1054–1061.
- [26] L. Richeldi, U. Costabel, M. Selman, et al., Efficacy of a tyrosine kinase inhibitor in idiopathic pulmonary fibrosis, *N. Engl. J. Med.* 365 (2011) 1079–1087.
- [27] N. Kazunori, O. Hideya, F. Akiko, et al., NFκB and TGFβ contribute to the expression of PTPN3 in activated human lymphocytes, *Cell. Immunol.* 358 (2020), 104237.
- [28] O. Yasuhiro, O. Hideya, K. Satoko, et al., Patched 1-interacting peptide represses fibrosis in pancreatic cancer to augment the effectiveness of immunotherapy, *J. Immunother.* 43 (2020) 121–133.
- [29] Philippe Lory, Sophie Nicole, Amaud Monteil, Neuronal Cav3 channelopathies: recent progress and perspectives, *Pflugers Arch. - Eur. J. Physiol.* 472 (2020) 831–844.
- [30] Qi-Wen Fan, Christine Cheng, Zachary A. Knight, et al. EGFR signals to mTOR through PKC and independently of Akt in glioma. *Sci Signal* 2(55): ra4.
- [31] L. Huia, L. Yana, Liu Xianhong, et al., A novel multi-target tyrosine kinase inhibitor anlotinib combined with irinotecan has in-vitro anti-tumor activity against human small-cell lung cancer, *Anticancer Drugs* 10 (2020) 1057–1064.
- [32] J. Vladimir, S. Ivan, K. Gordana, A comparison of the NK cell cytotoxicity with effects of TNF-alpha against K-562 cells, determined by LDH release assay, *Cancer Lett.* 138 (1–2) (1999) 67–72.
- [33] M. Gavrieli, N. Watanabe, S.K. Loftin, et al., Characterization of phosphotyrosine binding motifs in the cytoplasmic domain of B and T lymphocyte attenuator required for association with protein tyrosine phosphatase SHP-1 and SHP-2, *Biochem. Biophys. Res. Commun.* 312 (2003) 1236–1243.
- [34] T. Okazaki, S. Chikuma, Y. Iwai, et al., A rheostat for immune responses: the unique properties of PD-1 and their advantages for clinical application, *Nat. Immunol.* 14 (2013) 1212–1218.
- [35] Y.N. Chen, M.J. LaMarche, H.M. Chan, et al., Allosteric inhibition of SHP2 phosphatase inhibits cancers driven by receptor tyrosine kinases, *Nature* 535 (2016) 148–152.
- [36] G. Rota, C. Niogret, A.T. Dang, et al., Shp-2 is dispensable for establishing T cell exhaustion and for PD-1 signaling in vivo, *Cell Rep* 23 (2018) 39–49.